



Practical considerations for operability of an 8" spiral wound forward osmosis module: Hydrodynamics, fouling behaviour and cleaning strategy

Jungeun Kim ^{a,1}, Gaetan Blandin ^{c,1}, Sherub Phuntsho ^a, Arne Verliefde ^d, Pierre Le-Clech ^{b,*}, Hokyong Shon ^{a,*}

^a School of Civil and Environmental Engineering, University of Technology, Sydney, Post Box 129, Broadway, NSW 2007, Australia

^b UNESCO Centre for Membrane Science and Technology, School of Chemical Engineering, The University of New South Wales, Australia

^c LEQUIA, Institute of the environment, University of Girona, Campus Montilivi, Girona, Spain

^d Ghent University, Faculty of Bioscience Engineering, Department of Applied Analytical and Physical Chemistry, Particle and Interfacial Technology Group (PainT), Gent, Belgium

HIGHLIGHTS

- An 8" commercial spiral wound CTA and TFC FO modules were investigated.
- TFC module showed much higher permeability and selectivity in FO and PAO modes.
- Draw flow rate in the CTA modules must be operated at least 5 times lower than feed flow rate.
- In practice, feed pressure could be considered as an indicator of fouling occurrence.
- The combination of osmotic backwash and physical cleaning is effective for cleaning CTA and TFC modules.

ARTICLE INFO

Article history:

Received 10 June 2016

Received in revised form 1 November 2016

Accepted 4 November 2016

Available online 21 November 2016

Keywords:

Spiral wound module

Forward osmosis

Pressure-drop

Pressure assisted osmosis

Organic fouling

Osmotic backwash

ABSTRACT

A better understanding of large spiral wound forward osmosis (SW FO) module operation is needed to provide practical insight for a full-scale FO practical implementation desalination plant. Therefore, this study investigated two different 8" SW FO modules (i.e. cellulose tri acetate, CTA and thin film composite, TFC) in terms of hydrodynamics, operating pressure, water and solute fluxes, fouling behaviour and cleaning strategy. For both modules, a significantly lower flow rate was required in the draw channel than in the feed channel due to important pressure-drop in the draw channel and was a particularly critical operating challenge in the CTA module when permeate spacers are used. Under FO and pressure assisted osmosis (PAO, up to 2.5 bar) operations, the TFC module featured higher water flux and lower reverse salt flux than the CTA module. For both modules, fouling tests demonstrated that feed inlet pressure was more sensitive to foulant deposition than the flux, thus confirming that FO fouling deposition occurs in the feed channel rather than on the membrane surface. Osmotic backwash combined with physical cleaning used in this study confirmed to be effective and adapted to large-scale FO module operation.

© 2016 Elsevier B.V. All rights reserved.

1. Introduction

The most commonly used desalination technologies are generally pressure-based membrane processes such as reverse osmosis (RO) and nanofiltration (NF). However, the wider development of these processes is often limited due to high membrane fouling and scaling propensity and high energy consumption, resulting in operation and maintenance costs [1–3]. As a potentially more sustainable alternative,

the use of forward osmosis (FO) has been recently put forward and extensively investigated. In FO, the driving force is an osmotic pressure gradient, allowing water to naturally flow from a low chemical potential feed solution (FS) to a concentrated high chemical potential draw solution (DS) through a semipermeable membrane [4,5]. Although direct cost comparison of FO with conventional NF and RO systems remains a challenging task, several studies have demonstrated that desalination by FO could lead to lower energy consumption, reduced fouling propensity and higher cleaning efficiency [5–7].

Recent interest in FO applications has been particularly driven by the performance improvement offered by the latest generation of FO membranes. The improvements include higher water permeability, greater selectivity and rejection, smoother active layer surface allowing lower

* Corresponding authors.

E-mail addresses: p.le-clech@unsw.edu.au (P. Le-Clech), Hokyong.Shon-1@uts.edu.au (H. Shon).

¹ Jungeun Kim and Gaetan Blandin contributed equally to this work.

fouling propensity, and quite importantly, a specifically adapted porous support layer offering low internal concentration polarization (ICP) yet still appropriate mechanical support for practical operation [4,5]. The first commercially available and specifically tailored FO membranes, based on cellulose triacetate (CTA), were developed by Hydration Technology Innovations (HTI, Albany, OR), and have been examined in various applications by numerous research groups [8–13]. More recently, thin film composite (TFC) FO membranes were designed with a polyamide selective layer, and these feature higher water flux and better solute rejection compared to CTA membranes [14–17]. In addition, TFC membranes were found to be more pH stable and were more resistant to hydrolysis and biological degradation [17–19]. In contrast, previous studies have reported that TFC membranes showed higher fouling tendency than CTA membranes due to the increased surface roughness [17, 18,20,21]. As such opportunities to increase flux with commercially available membrane exists, but long-term fouling studies are required. An optimised FO module design is expected to feature high membrane packing density, lower concentration polarization (i.e., high mass transfer coefficient) and high water permeation [22]. Performance of several commercial FO membranes (i.e., Porifera and Toyobo) has been widely reported in the literature on small membrane samples but information regarding module design is still limited since most commercial FO membrane modules are still under development. Only the performance of SW FO modules developed by HTI has been reported for a variety of feed and draw spacers (fine, medium and corrugated spacer) [12] while detailed information on other suppliers module configurations are not available. This clearly indicates that CTA and TFC membrane modules were the most mature and developed membranes during the time of this FO study. In this regard, most studies so far were conducted using small flat sheet membrane coupons which are not always representative of behaviour in full-scale modules. Therefore, a better understanding of FO behaviour in larger modules is needed to provide more practical insight for full-scale FO operation.

A large-scale spiral wound (SW) FO module typically requires four ports: two inlets and two outlets for both the FS and DS. In SW FO modules, the FS circulates in the feed channel between the rolled layers, and the DS flows through the central tube into the inner side of the membrane envelop [23]. Therefore, flow patterns and flow resistance in the feed and draw channels can be different and affected by specific module design. In particular, a more detailed study linking operating conditions (flow rates, inlet pressures) to resulting performances (water flux, reverse salt flux, fouling and cleaning efficiency) of SW FO modules will provide important insights in the operability of current SW FO modules on full-scale.

Very limited pilot-scale FO studies using SW FO modules currently exist in literature [23–25]. However, these pilot studies are of crucial importance for further FO development since the operation of SW modules in industrial plants is affected by several factors such as the number of membrane leaves, feed and draw channel height, spacers that affect mass transfer and pressure loss, but also fouling potential [26]. To the best of the author's knowledge, so far only two studies have been reported in literature using 4040 SW (4" in diameter and 40" in length) [24] and 8040 SW (8040, 8" inch in diameter and 40" in length) [23] HTI CTA FO modules. Those studies mainly focused on the optimisation of a large-scale SW FO module [24] and of a newly proposed fertiliser drawn forward osmosis process for a specific application [23,27]. However, the susceptibility of SW FO modules to membrane fouling during the long-term FO operation has not been considered in those studies, which could consequently exacerbate the performance of in full-scale FO stand-alone or hybrid process. Although membrane fouling on the feed side in FO happens less and is easily removed by simple physical cleaning [3,28,29], the effect of osmotic backwash seems to be unclear. Some studies have reported that the osmotic backwash could lead to an adverse effect on the driving force due to the accumulation of the reversed solutes within the fouling layer [29–31]. Nevertheless, the specific combination of osmotic backwash with subsequent physical cleaning

could be more effective to restore a significant portion of water productivity after fouling occurred [32]. Thus, there is a critical need to control operating conditions and assess performances of SW FO modules more systematically including fouling behaviour and cleaning strategies for sustainable FO operation.

As an alternative to FO, a new FO-derived concept called pressure assisted osmosis (PAO) has recently been developed. PAO is aimed at increased water production compared to FO for more favourable economics for further commercialization [32–36]. In PAO, hydraulic pressure is applied on the feed side of the membrane to enhance the water flux through the synergistic effects of hydraulic pressure and osmotic pressure [32–36]. Overall, it has been demonstrated that by increasing the applied pressure, the water flux was significantly improved despite higher ICP. Even more than for FO, the role of a spacer in the PAO process is important to prevent the deformation and damage of the membrane caused by the applied hydraulic pressure on the feed side of the membrane [34,36,37]. This reinforces the need to evaluate the impact of hydraulic pressure on the module-scale FO and PAO operations.

Accordingly, there is a clear need for a detailed assessment of the impact of hydrodynamic conditions on pressure behaviour of an SW FO module (i.e. build-up in draw stream and drop along feed line). This study therefore systematically studied the performances of two commercial SW FO modules (CTA from HTI and TFC from Toray Industries Inc.). An assessment of the water flux and reverse salt flux behaviours as a function of operating conditions in both FO and PAO operation was conducted to evaluate the performance of both modules compared to lab-scale experiments. Fouling studies were performed with a mixture of model organic foulants was then used to evaluate the fouling behaviour and cleaning strategies for the modules operated in a seawater dilution application. To our best knowledge, this is the first study addressing the practical operations of commercially available 8" SW FO modules and providing a comparative assessment of long-term fouling behaviour in large-scale FO process. Therefore, the results reported in this study can be useful for further investigation of the fouling control by chemical cleaning and/or pre-treatment in full-scale FO operation.

2. Material and methods

2.1. Spiral wound FO membrane module

Two different 8" SW FO modules were used (Table 1): one CTA module manufactured by HTI and one TFC polyamide module manufactured by Toray Industries, Korea. In both modules, the rejection layer of the membrane faces the FS and the porous support layer of the membrane faces to the DS. Feed and permeate spacers were present to keep the membrane leaves apart [23,24].

As presented in Table 1, the CTA module had a corrugated feed spacer made of 2.5 mm polystyrene chevron and an effective membrane area of 9 m² with six membrane leaves. The TFC module had a feed spacer made of a 1.19 mm diamond type polypropylene mesh and an effective membrane area of 15 m² with ten membrane leaves. In addition, both modules had different permeate spacers: the CTA module had three tricot spacers, while the TFC module featured a draw channel containing one diamond type spacer wedged in between two tricot type spacers. If a net spacer is used inside of the envelope in the SW FO module and the DS side is pressurized, the feed flow channel may be blocked by membrane deformation. Accordingly, a tricot fabric spacer is used inside the envelope like a permeate carrier of an SW RO module and prevents the membrane deformation and this structure has been already utilised for pressure-retarded osmosis application [38]. Water permeability (A) for both FO modules was measured in RO mode in a pilot-scale FO unit (tap water - conductivity 240 ± 20 µm/cm - in the feed and draw sides). The tests were conducted at increasing feed pressures (in intervals of 0.5 bar up to 2.5 bar). A_{CTA} and A_{TFC} were found to be 1.6 ± 0.2 and 8.9 ± 0.14 Lm⁻² h⁻¹ bar⁻¹, respectively. Additional information on the properties of the CTA and TFC FO membranes such

as water and salt permeability (A and B values), feed rejection (R), structural parameter (S) and membrane total thickness are all provided in the Table S2 in the Supplementary Information.

2.2. Feed and draw solutions

A draw solution at a concentration of 35 g/L of Red Sea salt (RSS) from Red Sea Inc. with an equivalent osmotic pressure of 24.7 bar was prepared and used in all experiments [32,33]. RSS composition is described in Table S1 in the Supplementary Information. Humic acid and alginate were chosen as model organic foulants, while calcium (as calcium chloride, CaCl_2) was added to further enhance fouling. Model organic foulants used in this study have been known as major organic components in wastewater and have extensively been used to study in fouling behaviour in FO process [32,39,40]. In fouling experiments, the FS was prepared by mixing the following chemicals to tap water: 1.2 g/L RSS, 0.22 g/L CaCl_2 (Ajax Finechem Pty Ltd., Tarend point, Australia), 0.2 g/L humic acid sodium salt (Aldrich, Milwaukee, WIS) and 0.2 g/L alginic acid sodium salt (Sigma Aldrich Co., St Louis, MO). The total organic carbon (TOC) concentration of the feed was 94 mg/L. Before and after the fouling experiments, baseline experiments were conducted using tap water and 35 g/L RSS as FS and DS, respectively.

2.3. Pilot-scale system and experimental procedure

As shown in Fig. 1, a pilot-scale FO system was used for the experiments. Details about the design and control of the pilot-scale FO system are provided in our previous study [23]. Flow meters, pressure gauges and electrical conductivity (EC) meters were installed at both the inlet and outlet points of the module and connected to a computer for online data recording and monitoring. Although the feed and draw flow rates were varied between 17 and 100 L/min and between 4 and 15 L/min, respectively, the cross-flow velocity of each module shows difference due to their different module designs. The converted feed and draw cross-flow velocities for both are presented in Table 2.

The impact of feed and draw flow rates on pressure-drop were successively evaluated. For this evaluation, 500 L of FS and DS were prepared with tap water, and each experiment was carried out at a fixed draw flow rate, while the feed flow rate was varied and vice versa. Details of the experiment conditions are summarized in Table 2.

PAO operation was also tested to assess the effect of the hydraulic pressure in the feed channel. Feed pressure was changed by adjusting

the back pressure valve for fixed feed and draw flow rates. The maximum operating pressure used in this study was 2.5 bar as feed inlet pressure. The PAO experiments were performed with 200 L of 35 g/L RSS as DS and 500 L of tap water as FS. The feed and draw flow rates were constant and fixed based on the optimised conditions defined in the initial SW FO module experiments.

Water fluxes (J_w , $\text{L m}^{-2} \text{ h}^{-1}$) were calculated by using the following formula:

$$J_w = \left(\frac{\text{Change in DS volume (L)}}{A_m (\text{m}^2) \times \Delta t (\text{hr})} \right)$$

where A_m is the effective membrane surface area (m^2) and Δt is the operation time (hr). In addition, the recovery rate (%) during the operation in FO and PAO modes was defined as

$$\text{Recovery rate} = \frac{\text{Permeated volume (PV, L)}}{\text{Initial FS volume (L)}} \times 100$$

When tap water was used as FS in FO and PAO modes, the change in FS salt concentration (and thus reverse salt flux) was determined based on conductivity measurements (using a multimeter CP-500 L, ISTEK, Korea) [6]. The concentration change in the feed solution at the beginning and end of each experiment was measured. The measured value was used to calculate the specific reverse solute flux (SRSF), which is defined as a ratio of reverse salt flux (J_s , $\text{gm}^{-2} \text{ h}^{-1}$) and water flux (J_w , $\text{L m}^{-2} \text{ h}^{-1}$) [34,41]. SRSF (J_s/J_w , g/L) was then calculated using the following formula:

$$\text{SRSF} = \frac{1}{J_w} \left(\frac{C_f V_f - C_i V_i}{A_m \Delta t} \right)$$

where C_i and C_f are the initial and final feed solute concentration (g/L), and V_i and V_f are the initial and final volume of the feed water (L). When DI water was used as FS, the RSF/SRSF was determined by measuring the increased electrical conductivity of the FS between the start and end of each batch experiment. The electrical conductivity was then converted into mass concentration using calibration curve for the RSS concentration versus conductivity as shown in Fig. S1 in the Supplementary Information.

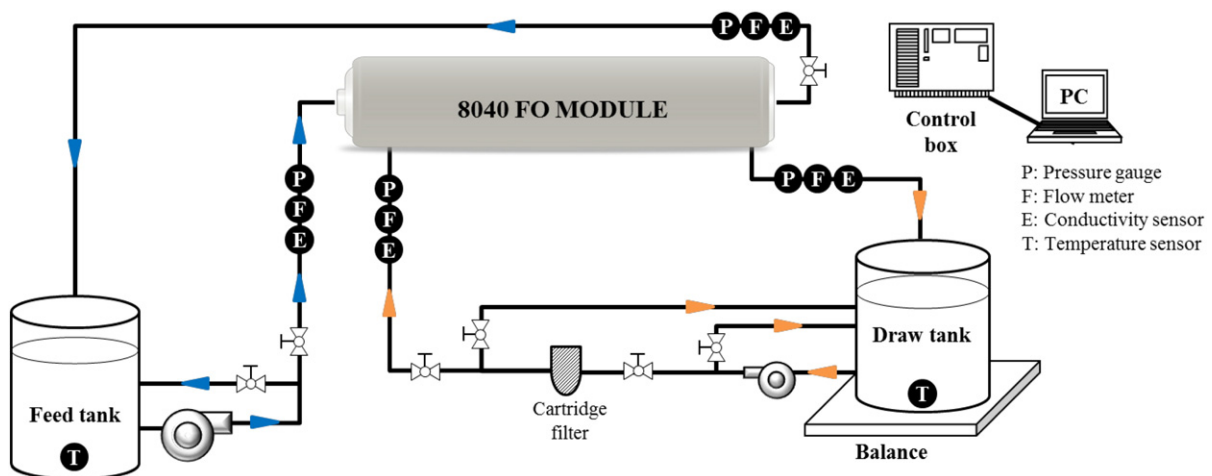


Fig. 1. Schematic diagram of the pilot-scale FO experimental set up and illustration of 8040 spiral wound FO modules: CS CTA and MS TFC (CS: corrugated feed spacer and MS: medium diamond shape feed spacer).

2.4. Fouling cycles and cleaning experimental procedure

Fouling behaviour was evaluated in FO operation (no hydraulic pressure added, i.e. back pressure valve opened) for both modules. All experiments were conducted with 200 L of 35 g/L RSS as DS and 500 L mixed fouling solution (as described in Section 2.2) as FS. After 400 L of water permeated (i.e. after 80% recovery feed water reached), the test was stopped and new feed and draw solutions were prepared and a new fouling cycle was initiated (without cleaning in-between cycles). Fouling runs were repeated for three cycles in total, before cleaning took place. Operation time for the CTA module was much longer than for the TFC module due to its low water permeability (since similar permeation volumes were aimed at).

Osmotic backwashing was conducted after the three fouling cycles, using 200 L of 35 g/L RSS as cleaning DS (replacing the feed water) and tap water as cleaning feed solution (replacing the DS) for 60 min to remove the fouling layer from the membrane surface at the same feed and draw flow rates of 40 and 10 L/min, respectively for both modules (cross-flow velocities for each module are shown in Table 1). After the osmotic backwash, physical cleaning at 100 L/min of feed flow rate (0.44 and 0.91 m/s for CTA and TFC modules, respectively) was performed for 5 min using tap water to flush the dislodged foulants from the feed channel [32]. During the physical cleaning, samples of the feed side (used as draw side during the backwashing) were collected every 1 min (100 L flushing), and analysed using a total organic carbon (TOC) analyser (SGE AnatoC TOC II Analyser). Before each fouling run, as well as before and after cleaning, the baseline flux was measured by operation with tap water as FS and 35 g/L as DS for 30 min to assess the

influence of fouling on membrane permeability and inlet pressure (and pressure-drop) in the feed channel.

3. Results and discussion

3.1. Impact of operating conditions on module hydrodynamics

3.1.1. Impact of feed and draw flow rates on pressure-drop (without permeation)

It should be noted that the flow rate range is much lower in the draw channel, as recommended in [23,24]. Results for the CTA module (Fig. 2(a)) indicate that the effect of feed flow rate increase on the pressure-drop was moderate (at constant draw cross-flow velocity of 0.04 m/s). When the feed cross-flow velocity was increased from 0.08 to 0.44 m/s, the feed inlet pressure was increased from 0.17 to 0.27 bar. In addition, as shown in Fig. 2(b), when the draw cross-flow velocity was increased from 0.03 to 0.05 m/s (much lower range than for feed stream), the draw inlet pressure was more linearly increased from 0.39 to 0.74 bar. This demonstrates that much higher flow resistance occurs in the draw channel of the CTA module, which is mainly due to the use of dense and thick draw tricot spacers with lower cross-flow velocities in both sides of the module (Table 1) [42].

When the feed cross-flow velocity was increased from 0.16 to 0.91 m/s in the TFC module (Fig. 2(c)), the feed inlet pressure was increased from 0.22 to 0.39 bar. Specifically, under much higher feed cross-flow velocity of 0.91 m/s (Table 1), the feed inlet pressure with the TFC module is slightly higher (0.39 bar) than that with the CTA module (0.27 bar), which corroborates with the fact that the spacer used in

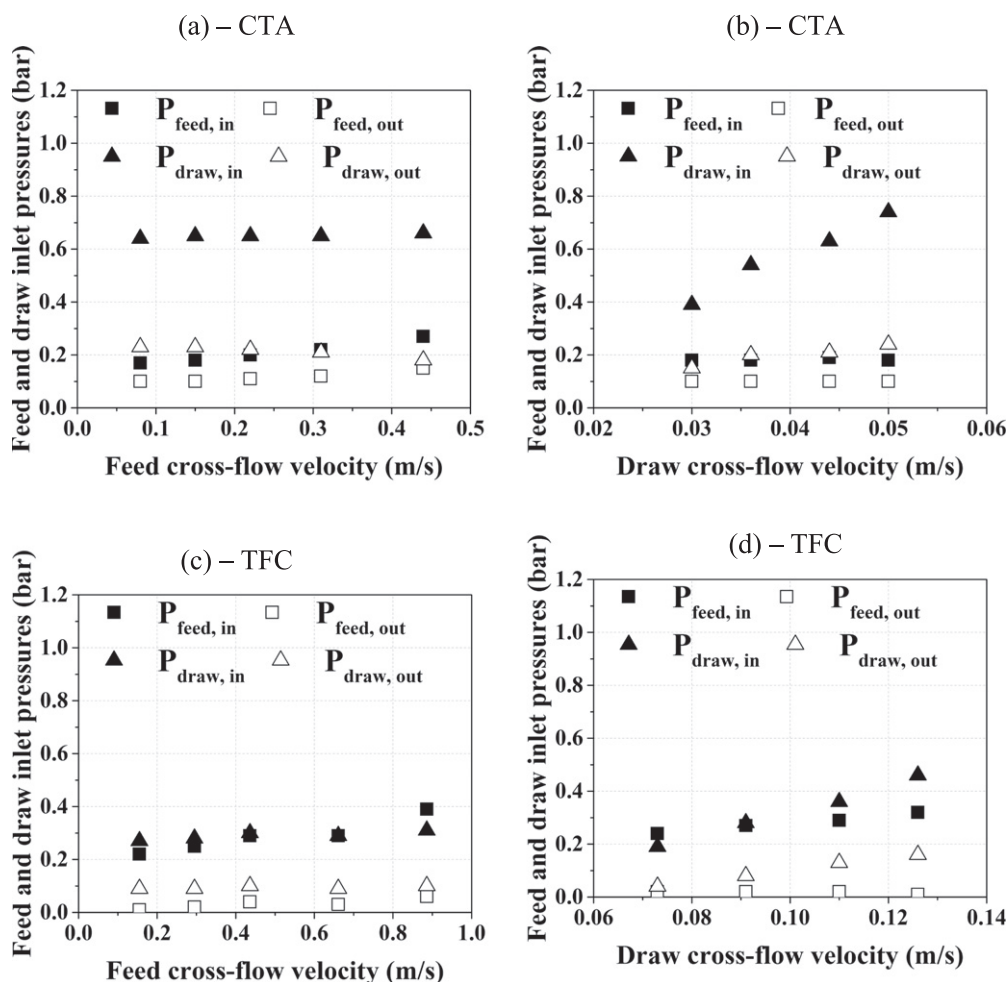
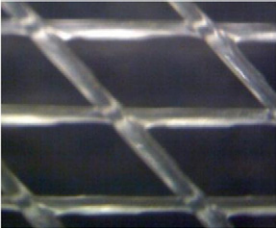
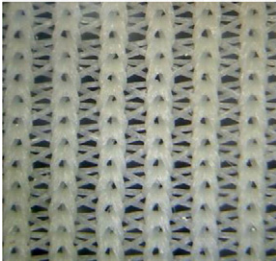
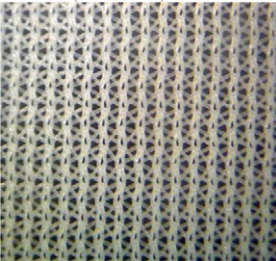


Fig. 2. Effect of feed and draw cross-flow velocities on pressure build-up in CTA (a and b) and TFC (c and d) modules. Tap water was used as FS and DS.

Table 1

Specifications of two spiral wound forward osmosis membrane modules employed in this study.

Parameter	CTA (HTI)	TFC (Toray)
Water permeability (A), $\text{Lm}^{-2} \text{h}^{-1} \text{bar}^{-1}$	1.6 ± 0.2	8.9 ± 0.1
Effective membrane area, m^2	9	15
Number of leaves in the assembly	6	10
Feed spacer thickness, mm	2.5	1.19
Feed spacer type	Corrugated polystyrene	Diamond polypropylene
^a Image of feed spacer	n.a.	
Draw spacer type	Tricot (dense/rigid)	Tricot (flexible)/diamond
^a Image of draw spacer		

^a Microscope measurement (5MP USB 2.0 Digital Microscope) and the spacers obtained from the SW FO module autopsy.

the feed channel of the TFC module is thinner (1.19 mm) with higher packing density leading to lower feed channel height (0.00258 mm for TFC and 0.00394 mm for CTA), resulting in higher feed inlet pressure [26,43,44]. Pressure-drop in the draw channel of the TFC module was not only lower but also much less sensitive to flow rate variation than in the CTA module, mainly due to the presence of one layer of diamond spacer with much lower resistance in the draw channel (Fig. 2(d)).

As such, it is clear that spacer design is of crucial importance for pressure-drop in the SW FO module. The tested CTA module with a corrugated spacer in the feed channel does allow a very low pressure drop in the feed channel, but this comes at the cost of a low packing density. Most likely, this is only justifiable economically if feed waters with a very high load of foulants and potential clogging problems is treated. In that aspect, the diamond spacer used in the TFC module appears to be a better compromise that allows for higher packing densities at moderate pressure drop. The permeate spacers used in the CTA module resulted in a very large pressure drop, even at low flow rate. Combinations of tricot permeate spacers to support the membrane and limit deformation and a diamond spacer to limit pressure-drop (as in the TFC module) allows using higher draw flow rates.

3.1.2. Impact of feed and draw channel pressurisation on pressure-drop

In these experiments, the system was operated by adjusting the feed inlet pressure using the back pressure valve of the feed side. Fig. 3 shows the impact of the feed inlet pressure on the feed and draw channel inlet and outlet pressures for both modules. For both modules (Fig. 3(a) and (b)), the draw inlet pressure was increased when pressure was applied

on the feed side. Interestingly, both modules have very distinct behaviour with regards to this “pressure transfer.” For the CTA module, the draw inlet pressure increase is already maximal at lower hydraulic pressures (1 bar), and remains constant even when further increasing the feed pressure (up to 2.5 bar). This appears to indicate that the pressurisation of the draw side in the CTA module is more likely a consequence of draw channel pressurisation on the tricot type support on the draw side. At higher pressures, further reduction of the channel is not possible as the tricot support could not be more compacted. For the TFC module, a more linear increase in the draw inlet pressure was observed with increasing feed pressure (Fig. 3(b)). Here, it could thus be hypothesized that the diamond type spacer is less supportive and allows for more channel reduction [33,45]. To identify the reason behind the increases in draw pressure for both modules, RO tests with the modules were compared to tests in FO mode (using tap water as FS and DS).

3.2. Relative contribution of hydraulic pressure to permeation flux

FO and PAO tests were carried out using CTA and TFC modules (Fig. 4), and now with tap water as FS, and 35 g/L RSS as DS. The water fluxes in FO and PAO modes with the TFC module were significantly higher than that with the CTA module. For example, in FO mode (no hydraulic pressure applied), the flux with the TFC module was around $16.6 \text{ Lm}^{-2} \text{h}^{-1}$, while the flux with the CTA module was around $5.4 \text{ Lm}^{-2} \text{h}^{-1}$. The higher performance of the TFC membranes compared to CTA membranes corroborates findings from literature [16,46].

Table 2

Experimental conditions for module hydrodynamic tests.

Module	Test no.	Feed cross-flow velocity, m/s (L/min)	Draw cross-flow velocity, m/s (L/min)	FS and DS
CTA	Test 1	0.08–0.44 (17–100)	0.04 (10)	Tap water of 500 L
	Test 2	0.18 (40)	0.02–0.07 (4–15)	
TFC	Test 3	0.16–0.91 (17–100)	0.09 (10)	
	Test 4	0.37 (40)	0.04–0.14 (4–15)	

In PAO mode (Fig. 4), as expected, the water flux improved with increasing applied pressures. For the CTA module, the flux increase with applied pressure was moderate, i.e., from 6.72 to $7.3 \text{ Lm}^{-2} \text{ h}^{-1}$ (at 2.5 bars of applied pressure) and remained much lower than the fluxes obtained with the TFC module. For the TFC module, the impact of the applied pressure on the water flux was significant, already at low applied pressure (flux increased from 19 to $24.5 \text{ Lm}^{-2} \text{ h}^{-1}$ at 1 and 2.5 bar, respectively). This confirms that the TFC membranes not only has higher permeation flux in FO mode, but is also more responsive to the use of hydraulic pressure (PAO mode) due to its higher water permeability. Although additional energy is required to pressurise the feed solution in PAO, the significant increase in performance could lead to additional cost savings, in particular by a reduction of the number of membrane modules required [47].

Table 3 shows the comparison of the specific reverse salt flux (SRSF) behaviour for FO and PAO modes using the two different SW FO modules. Compared to the CTA module, the TFC module had much lower SRSF, and thus not only had a higher flux but also a higher selectivity than the CTA module. As expected from the previous lab experiments, the results show a significant decrease in the SRSF for both modules with increasing applied pressure. For example, the SRSF were 1.22 and 0.37 g/L for CTA and TFC, respectively in FO mode, and decreased down to 0.64 and 0.10 g/L for CTA and TFC, respectively in PAO mode with a feed inlet pressure of 2.5 bar [33,34,36]. This corroborates previous findings that reverse transport of the draw solutes through the membranes is significantly decreased by the enhanced water permeation. The effect of hydraulic pressure on the RSF for the TFC is even more propounded compared to the CTA, due to the higher water permeability of the TFC. Also, the CTA module could have the risk of irreversible fouling on the support layer caused by more solute diffusing from DS into FS in which the enhanced salt accumulation on the feed side of the CTA module and is mainly promoted by the reverse diffusion of Na^+ [48,49]. Such reverse solute flux through the FO membranes can have significant economic impact on the FO process. Draw solute leakages through SRSF in the FO process is one of the major contributors to draw solute replenishment cost in a continuous closed-loop configuration [50]. A recent study conducted by Phuntsho et al. [51] has pointed out that accumulation of draw solutes in the feed brine would be one of the significant environmental challenges for brine disposal, especially for FO membranes with lower reverse flux selectivity. This indicates that, CTA with lower reverse flux selectivity (as shown in Table 3) would result in much higher accumulation of draw solutes in the feed brine thus leading to higher draw replenishment and brine treatment costs. These studies clearly show that the TFC FO membrane with much higher reverse flux selectivity than CTA FO membrane would be more beneficial for FO hybrid systems.

3.3. Fouling behaviour in SW FO modules and impact on hydraulic performance

The water flux as a function of permeate volume is presented in Fig. 5(a) and (c) while permeate volume and recovery rate as a function of operation time is shown in Fig. 5(b) and (d). During each batch, flux decreased significantly with time (and increasing recovery) due to a combination of the osmotic dilution of the DS and potentially fouling.

Only when comparing initial permeation fluxes for batches, occurrence of fouling can be individually assessed. No significant initial permeation flux decline with batches was observed for neither of the tested modules, even after three batches of operation without cleaning in between. As such, despite the relative long time of operation, especially for the CTA module, and the high load of foulant used, a faster flux decline was noticed at early stages of operation but between fouling experiments the flux decline was relatively small (Fig. 5(a)). For the TFC module (Fig. 5(b)), fouling was limited, although a higher impact of fouling was initially expected due to the higher roughness of the membrane and the higher permeation flow compared to the CTA [1,52]. Such little flux decline for TFC module shows that the fouling happening in the SW FO module is clearly different from the results reported in existing literature, which was conducted using small FO membrane coupons [21,53,54]. This study seems to suggest that the membrane surface properties play a less dominant role in SW FO module fouling.

Nevertheless, there was the steep decrease of the initial water flux was observed with CTA module, and the initial recovery rate between the CTA and TFC modules was significantly different (recovery rate of 10% and 2% for CTA and TFC modules, respectively), resulting in the huge difference of operation time for CTA and TFC modules (i.e. 20 times higher). This was more likely because of two reasons; the impact of ECP on the membrane surface of the CTA module mainly due to higher RSF (discussed in Section 3.2) and that the CTA module used in this study has been operating several times before we conducted the fouling experiments, thus it could already have a fouling layer on the membrane surface to some extent even though the flux was almost fully restored after hydraulic cleaning [51]. More specifically, it was observed that the recovery rate of the CTA module after 10 h operation was around 1% with water flux of lower than $1 \text{ Lm}^{-2} \text{ h}^{-1}$ and thus there was no meaning to operate CTA module longer than 10 h (Fig. 5(a)). From this aspect, CTA and TFC module configuration in a full-scale FO desalination plant cannot be the same and it is dependent on the performance of FO membrane modules. Thus, it is more preferred that CTA modules should be paralleled in a full-scale FO desalination plant.

To get further insight in the behaviour of the SW FO modules during the fouling (as no real decrease in water permeability was noticed over the bathes), feed inlet pressure was compared before and after the fouling experiments. Fig. 6 compares the feed inlet pressure during fouling experiments with the feed pressure using pure water as feed before and after the third batch of fouling. As shown in Fig. 6, as soon as the foulant mixture was used as FS, a much higher feed inlet pressure was observed in the module, due to higher viscosity resulting in an increase flow resistance and pressure-drop along the membrane channel on the feed side. This feed pressure increase most likely indicates foulant deposition, although no decrease in permeation flux was noticed. This would indicate that fouling occurs more in the channel spacers rather than on the membrane surface. Most likely, the foulants accumulated in dead zone of the feed spacer, and consequently, the cross-flow velocity and the required pressure increased in the feed channel. Despite the fact that no decrease in membrane water permeability is seen, the increased pressure-drop in the feed channel is of course unwanted. Increased pressure drops lead to higher energy consumption for the pump to maintain the water circulation [26]. As such, controlling fouling in the

Table 3

Comparison of specific reverse salt flux (SRSF, J_s/J_w) behaviour in pilot-scale FO and PAO processes using two different SW FO modules: CTA and TFC.

Operation mode	CTA module			TFC module		
	$J_{w, \text{CTA}} (\text{Lm}^{-2} \text{ h}^{-1})$	$J_{s, \text{CTA}} (\text{gm}^{-2} \text{ h}^{-1})$	$J_s/J_w (\text{g/L})$	$J_{w, \text{TFC}} (\text{Lm}^{-2} \text{ h}^{-1})$	$J_{s, \text{TFC}} (\text{gm}^{-2} \text{ h}^{-1})$	$J_s/J_w (\text{g/L})$
FO	5.4	6.58	1.22	16.6	6.1	0.37
PAO	1 bar	6.7	6.12	19.0	4.1	0.22
	2 bar	7.1	5.47	23.6	2.6	0.11
	2.5 bar	7.3	4.66	24.5	2.5	0.10

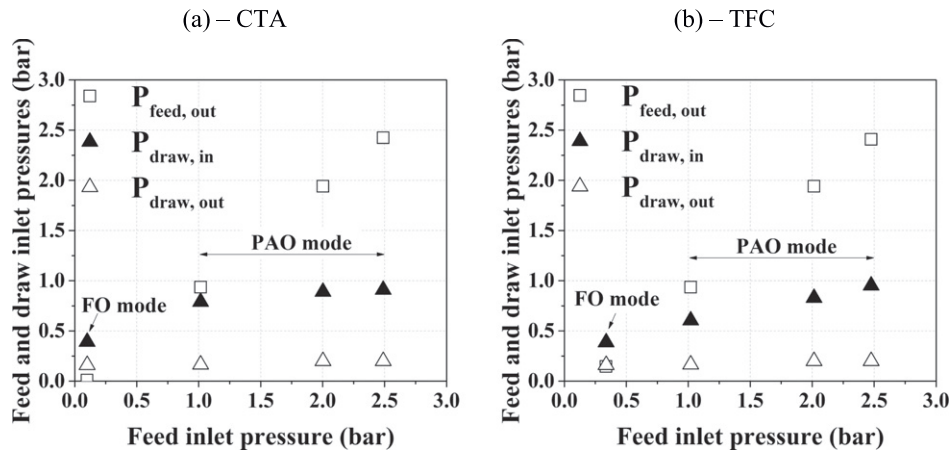


Fig. 3. Impact of feed inlet pressure on the feed and draw channel pressurisation with (a) CTA and (b) TFC modules. Feed cross-flow velocity was constant at 0.18 m/s for CTA and 0.37 m/s for TFC, while the draw flow cross-flow velocities for CTA and TFC modules were 0.04 and 0.09 m/s, respectively. Tap water was used as FS and DS.

feed channel, and avoiding unwanted pressure-drop will be a key parameter for real-life FO operation, especially on challenging feed streams. By comparing feed pressure (with tap water as FS) before and after fouling experiments, it is clear that for the TFC module, pressure-drop increased much more than for the CTA one (i.e. 1 and 0.25 bar, respectively). As discussed earlier, the corrugated spacer used in the CTA module leads to an increased channel thickness with lower initial pressure-drop and most likely less sensitivity to fouling deposition with much longer operation time. In addition, since the CTA module has shown lower cross-flow velocity of around 0.18 m/s compared to the TFC module (0.37 m/s) corresponding to the flow rate of 40 L/min, thus showing that mass transfer coefficient of TFC module (3.04×10^{-5} m/s) is higher than that of CTA module (2.40×10^{-5} m/s). Consequently, the loose fouling layer in the corrugated spacer can be flushed to some extent or changed by hydrodynamics due to its spacer geometry (Fig. 6).

3.4. Fouling reversibility by osmotic backwash

As discussed in Section 3.3, no significant impact of fouling was observed on permeation flux, indicating that fouling occurs more in the spacers rather than on the membrane surface in the SW FO modules. Therefore, it is unclear whether osmotic backwashing will have a clear effect on fouling remediation. To assess this, not only the water

permeability was monitored, but also the potential recovery of the pressure-drop in the feed channel. The cleaning strategy consisted in a combination of osmotic backwash followed by feed channel water flushing at high cross flow velocity (Section 2.4). During the osmotic backwash, the feed pressure drop remained relatively constant for the CTA module, but was observed to decrease slightly for the TFC module (see Fig. 7(a)). This indicates that the osmotic backwashing could be efficient to recover materials accumulated in the feed channel during operation, especially for TFC membrane module. Besides, as shown in Fig. 7(a), significant reverse flux difference between CTA and TFC modules was observed during the osmotic backwash. For instance, the reverse water permeation in the TFC module (average of $14.5 \text{ Lm}^{-2} \text{ h}^{-1}$) was much higher than that in the CTA module (average of $2.8 \text{ Lm}^{-2} \text{ h}^{-1}$), indicating that reverse flux assisted dissociation and dislodging of the foulant layer from the membrane surface could be more pronounced in the TFC FO membrane modules. The results in Fig. 7(b) therefore have confirmed that the feed inlet pressure was dramatically decreased after osmotic backwashing and flushing the feed channel under the highest cross flow velocity for each module, i.e. from 1.4 to 0.8 and from 0.35 to 0.25 for TFC and CTA modules, respectively. Still, the feed pressure was not restored to its original level for the clean module, thus indicating that almost full recovery was achieved or modification of the pressure balance in the module happened.

In order to compare the efficiency of the cleaning and estimate required durations for both modules, TOC concentrations flushed out of the module after each minute (i.e. 100 L) are presented in Fig. 7(c). The results indicate that a very high load of foulants is removed in the early stage of physical cleaning and after 3 min (300 L), the TOC level returns to that of the incoming tap water and no more foulants are flushed out the module. As such, it is clear that for the foulants used in this study, only a very short period of physical cleaning is required after osmotic backwash. Consequently, the combination of osmotic backwash and physical cleaning has proven to be an efficient cleaning strategy for the SW FO modules.

4. Conclusions

This study presented practical considerations of SW FO modules with different membrane properties (CTA and TFC). The evaluation of two modules was conducted to establish hydrodynamic conditions under different feed and draw flow rates. In addition, the performances of two SW FO modules under different operation modes (FO and PAO modes) were compared. Finally, the effectiveness of the combined

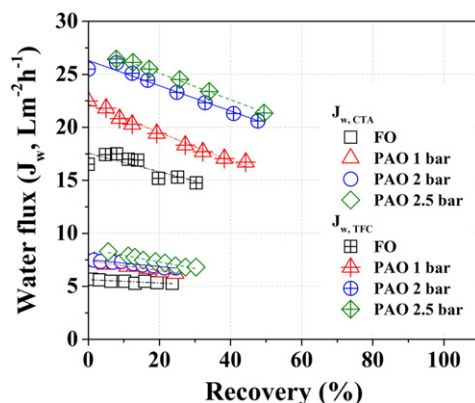


Fig. 4. Comparison of flux behaviour in pilot-scale FO and PAO processes using two different SW FO modules. Experimental conditions: feed flow rate: 0.18 and 0.37 m/s for CTA and TFC, respectively, draw flow rate: 0.04 m/s for CTA and 0.09 m/s for TFC, and applied pressure in PAO: 1, 2 and 2.5 bar, 35 g/L RSS as DS and tap water as FS.

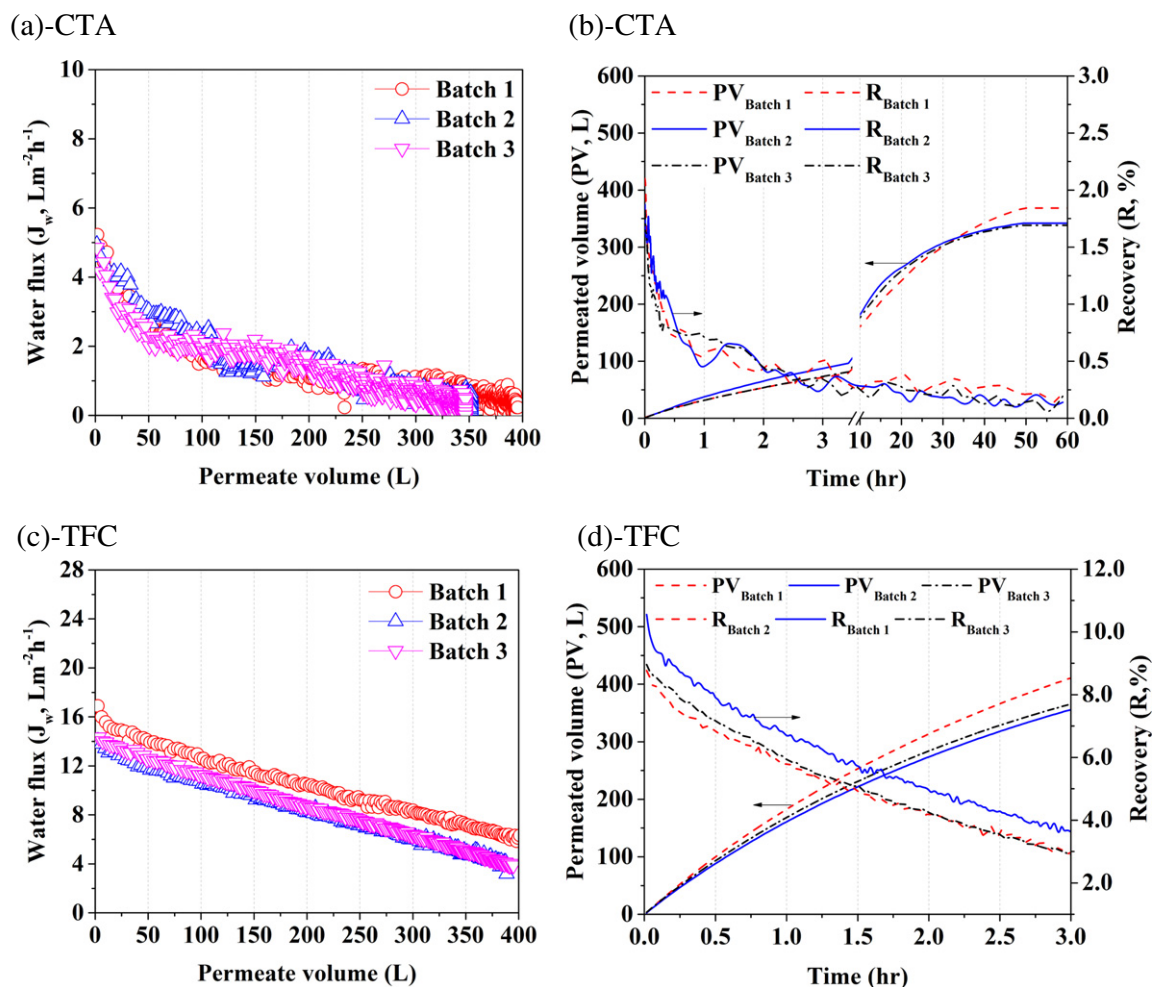


Fig. 5. Effect of organic foulant in feed solution on FO fouling of CTA (a and b) and TFC (c and d) modules. (a) and (c) water flux (J_w) as a function of permeate volume (L); (b) and (d) permeate volume (L) and recovery rate (R) as a function of operation time. Fouling experiments were conducted using 35 g/L RSS as DS and feed fouling solution prepared by addition of 1.2 g/L RSS, 0.22 g/L CaCl_2 , 0.2 g/L alginate, 0.2 g/L humic acid.

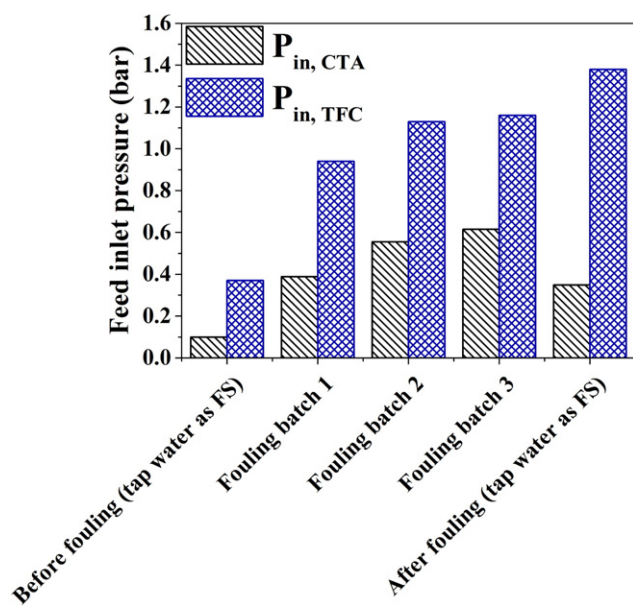


Fig. 6. Feed inlet pressure change with CTA and TFC modules. Fouling experiments were conducted using 35 g/L RSS as DS and feed fouling solution prepared by addition of 1.2 g/L RSS, 0.22 g/L CaCl_2 , 0.2 g/L alginate, 0.2 g/L humic acid.

osmotic backwash and physical cleaning on the flux recovery was evaluated. The following conclusions are drawn:

- The draw side of the CTA module was more sensitive to flow rate due to the use of permeate spacers thick tricot creating more resistance to the flux. The operation of the draw side of the TFC module is less restrictive thanks to a mesh spacer but then less mechanical support is provided to the feed stream in the module. Also, pressure transfer from the feed to the draw channel was observed in PAO operation due to the potential compaction and narrowing of the draw channel.
- Novel TFC membranes allow for higher permeation flux and is more responsive to hydraulic pressure (PAO)
- In PAO mode, enhanced water permeation caused by the additional hydraulic pressure on the feed side of the TFC module led to less RSF which is beneficial for process efficiency and potentially to limit (RSF enhanced) fouling propensity.
- Fouling tests demonstrated that fouling occurs even when only limited impact on permeation is observed. Pressure-drop can be an important indicator of fouling occurrence for practical SW FO operation.
- The combination of osmotic backwash and physical cleaning confirmed to be very efficient and easy to implement on a module scale. Nevertheless, it has to be acknowledged that further studies of effective cleaning strategies for FO process including chemical cleaning have to be conducted for improvement of techno-economic assessment of FO by evaluating organic removal efficiency and feed inlet pressure recovery.

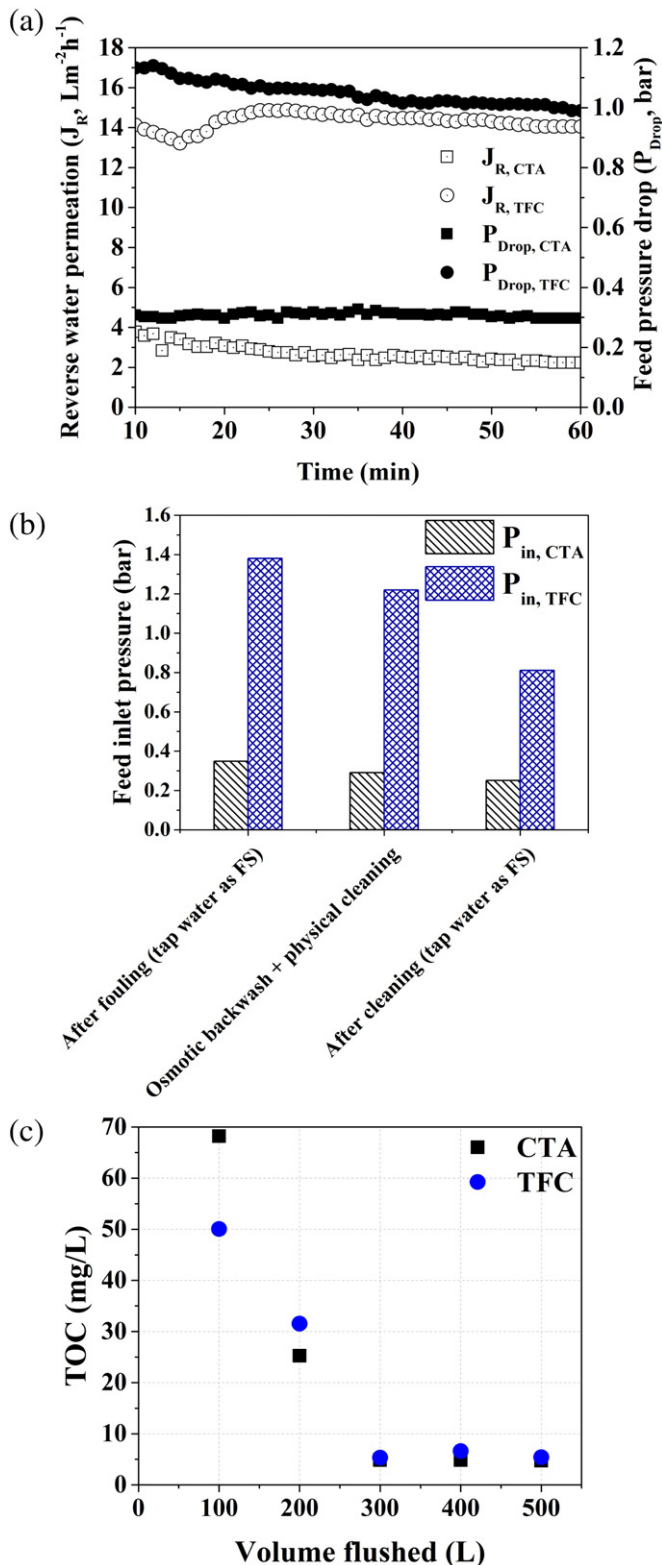


Fig. 7. (a) Variation of reverse water flux and feed pressure drop with osmotic backwash operation time, (b) effect of osmotic backwash and physical cleaning on the feed inlet pressure recovery and (c) total organic carbon (TOC, mg/L) concentration as a function of the water volume flushed (L). Physical cleaning with maximum feed cross-flow velocity of 0.44 and 0.91 m/s for CTA and TFC, respectively was performed for 5 min using tap water. The TOC of the feed was around 94 mg/L.

Although this study demonstrated that the application of PAO operation enables to enhance the water flux and to limit the RSF in both SW FO modules, further studies on the comprehensive assessment of the PAO process including long-term operations are required. This can help to define optimal design for FO and PAO processes to prevent the pressure and energy losses caused by fouling in the system.

Acknowledgements

The authors acknowledge the financial support of the National Centre of Excellence in Desalination Australia, which is funded by the Australian Government through the National Urban Water and Desalination Plan. This research was also supported by a grant (code 16IFIP-B088091-03) from Industrial Facilities & Infrastructure Research Program funded by Ministry of Land, Infrastructure and Transport of Korean Government. The research leading to these results has received funding from the People Programme (Marie Curie Actions) of the European Union Seventh Framework Programme (FP7/2007-2013) under REA grant agreement n° 600388 (TECNIOspring programme), and from the Agency for Business Competitiveness of the Government of Catalonia, ACCIÓ. Finally, the authors thank Hydration Technology Innovations and Toray chemical Korea Inc. for the 8040 FO membrane modules they provided.

Appendix A. Supplementary data

Supplementary data to this article can be found online at <http://dx.doi.org/10.1016/j.desal.2016.11.004>.

References

- [1] Q. She, R. Wang, A.G. Fane, C.Y. Tang, Membrane fouling in osmotically driven membrane processes: a review, *J. Membr. Sci.* 499 (2016) 201–233.
- [2] S. Phuntsho, F. Lotfi, S. Hong, D.L. Shaffer, M. Elimelech, H.K. Shon, Membrane scaling and flux decline during fertiliser-drawn forward osmosis desalination of brackish groundwater, *Water Res.* 57 (2014) 172–182.
- [3] S. Lee, C. Boo, M. Elimelech, S. Hong, Comparison of fouling behavior in forward osmosis (FO) and reverse osmosis (RO), *J. Membr. Sci.* 365 (1–2) (2010) 34–39.
- [4] S. Zhao, L. Zou, C.Y. Tang, D. Mulcahy, Recent developments in forward osmosis: opportunities and challenges, *J. Membr. Sci.* 396 (2012) 1–21.
- [5] T. Cath, A. Childress, M. Elimelech, Forward osmosis: principles, applications, and recent developments, *J. Membr. Sci.* 281 (1–2) (2006) 70–87.
- [6] S. Phuntsho, H.K. Shon, S. Hong, S. Lee, S. Vigneswaran, A novel low energy fertilizer driven forward osmosis desalination for direct fertigation: evaluating the performance of fertilizer draw solutions, *J. Membr. Sci.* 375 (1–2) (2011) 172–181.
- [7] J.R. McCutcheon, R.L. McGinnis, M. Elimelech, A novel ammonia-carbon dioxide forward (direct) osmosis desalination process, *Desalination* 174 (1) (2005) 1–11.
- [8] Phuntsho, S., A novel fertiliser drawn forward osmosis desalination for fertigation. (Doctoral Dissertation) 2012.
- [9] J.R. McCutcheon, R.L. McGinnis, M. Elimelech, Desalination by ammonia-carbon dioxide forward osmosis: influence of draw and feed solution concentrations on process performance, *J. Membr. Sci.* 278 (1–2) (2006) 114–123.
- [10] C.H. Tan, H.Y. Ng, A novel hybrid forward osmosis-nanofiltration (FO-NF) process for seawater desalination: draw solution selection and system configuration, *Desalin. Water Treat.* 13 (1–3) (2010) 356–361.
- [11] A. Alturki, J. McDonald, S.J. Khan, F.I. Hai, W.E. Price, L.D. Nghiem, Performance of a novel osmotic membrane bioreactor (OMBR) system: flux stability and removal of trace organics, *Bioresour. Technol.* 113 (2012) 201–206.
- [12] G. Blandin, A. Verliefde, J. Comas, I. Rodriguez-Roda, P. Le-Clech, Efficiently combining water reuse and desalination through forward osmosis–reverse osmosis (FO-RO) hybrids: a critical review, *Membranes* 6 (3) (2016) 37.
- [13] Y. Kim, L. Chekli, W.-G. Shim, S. Phuntsho, S. Li, N. Ghaffour, T. Leiknes, H.K. Shon, Selection of suitable fertilizer draw solute for a novel fertilizer-drawn forward osmosis–anaerobic membrane bioreactor hybrid system, *Bioresour. Technol.* 210 (2016) 26–34.
- [14] R. Wang, L. Shi, C.Y. Tang, S. Chou, C. Qiu, A.G. Fane, Characterization of novel forward osmosis hollow fiber membranes, *J. Membr. Sci.* 355 (1–2) (2010) 158–167.
- [15] J. Wei, C. Qiu, C.Y. Tang, R. Wang, A.G. Fane, Synthesis and characterization of flat-sheet thin film composite forward osmosis membranes, *J. Membr. Sci.* 372 (1–2) (2011) 292–302.
- [16] N.Y. Yip, A. Tiraferri, W.A. Phillip, J.D. Schiffman, M. Elimelech, High performance thin-film composite forward osmosis membrane, *Environ. Sci. Technol.* 44 (10) (2010) 3812–3818.
- [17] Y. Gu, Y.-N. Wang, J. Wei, C.Y. Tang, Organic fouling of thin-film composite polyamide and cellulose triacetate forward osmosis membranes by oppositely charged macromolecules, *Water Res.* 47 (5) (2013) 1867–1874.

- [18] Z. Wang, J. Tang, C. Zhu, Y. Dong, Q. Wang, Z. Wu, Chemical cleaning protocols for thin film composite (TFC) polyamide forward osmosis membranes used for municipal wastewater treatment, *J. Membr. Sci.* 475 (2015) 184–192.
- [19] G.M. Geise, H.S. Lee, D.J. Miller, B.D. Freeman, J.E. McGrath, D.R. Paul, Water purification by membranes: the role of polymer science, *J. Polym. Sci. B Polym. Phys.* 48 (15) (2010) 1685–1718.
- [20] X. Zhu, M. Elimelech, Colloidal fouling of reverse osmosis membranes: measurements and fouling mechanisms, *Environ. Sci. Technol.* 31 (12) (1997) 3654–3662.
- [21] E.M. Vrijenhoek, S. Hong, M. Elimelech, Influence of membrane surface properties on initial rate of colloidal fouling of reverse osmosis and nanofiltration membranes, *J. Membr. Sci.* 188 (1) (2001) 115–128.
- [22] K. Luttmiah, A.R.D. Verliefde, K. Roest, L.C. Rietveld, E.R. Cornelissen, Forward osmosis for application in wastewater treatment: a review, *Water Res.* 58 (2014) 179–197.
- [23] J.E. Kim, S. Phuntsho, F. Lotfi, H.K. Shon, Investigation of pilot-scale 8040 FO membrane module under different operating conditions for brackish water desalination, *Desalin. Water Treat.* 53 (10) (2014) 2782–2791.
- [24] Y.C. Kim, S.J. Park, Experimental study of a 4040 spiral-wound forward-osmosis membrane module, *Environ. Sci. Technol.* 45 (18) (2011) 7737–7745.
- [25] R.L. McGinnis, N.T. Hancock, M.S. Nowosielski-Slepown, G.D. McGurgan, Pilot demonstration of the NH_3/CO_2 forward osmosis desalination process on high salinity brines, *Desalination* 312 (2012) 67–74.
- [26] J. Schwinge, P.R. Neal, D.E. Wiley, D.F. Fletcher, A.G. Fane, Spiral wound modules and spacers: review and analysis, *J. Membr. Sci.* 242 (1–2) (2004) 129–153.
- [27] S. Phuntsho, H. Shon, S. Hong, S. Lee, S. Vigneswaran, J. Kandasamy, Fertiliser drawn forward osmosis desalination: the concept, performance and limitations for fertigation, *Rev. Environ. Sci. Biotechnol.* 11 (2) (2012) 147–168.
- [28] N.T. Hancock, P. Xu, M.J. Roby, J.D. Gomez, T.Y. Cath, Towards direct potable reuse with forward osmosis: technical assessment of long-term process performance at the pilot scale, *J. Membr. Sci.* 445 (2013) 34–46.
- [29] R. Valladares Linares, Z. Li, V. Yangali-Quintanilla, Q. Li, G. Amy, Cleaning protocol for a FO membrane fouled in wastewater reuse, *Desalin. Water Treat.* 51 (25–27) (2013) 4821–4824.
- [30] R. Valladares Linares, Z. Li, M. Abu-Ghdaib, C.-H. Wei, G. Amy, J.S. Vrouwenvelder, Water harvesting from municipal wastewater via osmotic gradient: an evaluation of process performance, *J. Membr. Sci.* 447 (2013) 50–56.
- [31] E. Arkhangelsky, F. Wicaksana, S. Chou, A.A. Al-Rabiah, S.M. Al-Zahrani, R. Wang, Effects of scaling and cleaning on the performance of forward osmosis hollow fiber membranes, *J. Membr. Sci.* 415–416 (2012) 101–108.
- [32] G. Blandin, A.R. Verliefde, P. Le-Clech, Pressure enhanced fouling and adapted anti-fouling strategy in pressure assisted osmosis (PAO), *J. Membr. Sci.* 493 (2015) 557–567.
- [33] G. Blandin, A.R.D. Verliefde, C.Y. Tang, A.E. Childress, P. Le-Clech, Validation of assisted forward osmosis (AFO) process: impact of hydraulic pressure, *J. Membr. Sci.* 447 (2013) 1–11.
- [34] S. Sahebi, S. Phuntsho, J.E. Kim, S. Hong, H.K. Shon, Pressure assisted fertiliser drawn osmosis process to enhance final dilution of the fertiliser draw solution beyond osmotic equilibrium, *J. Membr. Sci.* 481 (2015) 63–72.
- [35] K. Luttmiah, D.J.H. Harmsen, B.A. Wols, L.C. Rietveld, Q. Jianjun, E.R. Cornelissen, Continuous and discontinuous pressure assisted osmosis (PAO), *J. Membr. Sci.* 476 (2015) 182–193.
- [36] Y. Oh, S. Lee, M. Elimelech, S. Lee, S. Hong, Effect of hydraulic pressure and membrane orientation on water flux and reverse solute flux in pressure assisted osmosis, *J. Membr. Sci.* 465 (2014) 159–166.
- [37] J. Duan, E. Litwiler, I. Pinnau, Solution-diffusion with defects model for pressure-assisted forward osmosis, *J. Membr. Sci.* 470 (2014) 323–333.
- [38] Y.C. Kim, Y. Kim, D. Oh, K.H. Lee, Experimental investigation of a spiral-wound pressure-retarded osmosis membrane module for osmotic power generation, *Environ. Sci. Technol.* 47 (6) (2013) 2966–2973.
- [39] C. Boo, M. Elimelech, S. Hong, Fouling control in a forward osmosis process integrating seawater desalination and wastewater reclamation, *J. Membr. Sci.* 444 (2013) 148–156.
- [40] W.S. Ang, S. Lee, M. Elimelech, Chemical and physical aspects of cleaning of organic-fouled reverse osmosis membranes, *J. Membr. Sci.* 272 (1) (2006) 198–210.
- [41] W.A. Phillip, J.S. Yong, M. Elimelech, Reverse draw solute permeation in forward osmosis: modeling and experiments, *Environ. Sci. Technol.* 44 (13) (2010) 5170–5176.
- [42] A. Cipollina, G. Micale, Sustainable Energy from Salinity Gradients, Woodhead Publishing, 2016.
- [43] M. Shakaib, S. Hasani, M. Mahmood, Study on the effects of spacer geometry in membrane feed channels using three-dimensional computational flow modeling, *J. Membr. Sci.* 297 (1) (2007) 74–89.
- [44] M. Park, J.H. Kim, Numerical analysis of spacer impacts on forward osmosis membrane process using concentration polarization index, *J. Membr. Sci.* 427 (2013) 10–20.
- [45] Y.C. Kim, M. Elimelech, Adverse impact of feed channel spacers on the performance of pressure retarded osmosis, *Environ. Sci. Technol.* 46 (8) (2012) 4673–4681.
- [46] B.D. Coday, D.M. Heil, P. Xu, T.Y. Cath, Effects of transmembrane hydraulic pressure on performance of forward osmosis membranes, *Environ. Sci. Technol.* 47 (5) (2013) 2386–2393.
- [47] G. Blandin, A.R. Verliefde, C.Y. Tang, P. Le-Clech, Opportunities to reach economic sustainability in forward osmosis–reverse osmosis hybrids for seawater desalination, *Desalination* 363 (2015) 26–36.
- [48] M. Xie, L.D. Nghiem, W.E. Price, M. Elimelech, Impact of humic acid fouling on membrane performance and transport of pharmaceutically active compounds in forward osmosis, *Water Res.* 47 (13) (2013) 4567–4575.
- [49] B. Mi, M. Elimelech, Chemical and physical aspects of organic fouling of forward osmosis membranes, *J. Membr. Sci.* 320 (1–2) (2008) 292–302.
- [50] A. Achilli, T.Y. Cath, A.E. Childress, Selection of inorganic-based draw solutions for forward osmosis applications, *J. Membr. Sci.* 364 (1) (2010) 233–241.
- [51] S. Phuntsho, J.E. Kim, M.A.H. Johir, S. Hong, Z. Li, N. Ghaffour, T. Leiknes, H.K. Shon, Fertiliser drawn forward osmosis process: pilot-scale desalination of mine impaired water for fertigation, *J. Membr. Sci.* 508 (2016) 22–31.
- [52] G. Blandin, H. Vervoort, P. Le-Clech, A.R.D. Verliefde, Fouling and cleaning of high permeability forward osmosis membranes, *J. Water Process. Eng.* 9 (2016) 161–169.
- [53] B. Mi, M. Elimelech, Organic fouling of forward osmosis membranes: fouling reversibility and cleaning without chemical reagents, *J. Membr. Sci.* 348 (1) (2010) 337–345.
- [54] C.Y. Tang, Q.S. Fu, C.S. Criddle, J.O. Leckie, Effect of flux (transmembrane pressure) and membrane properties on fouling and rejection of reverse osmosis and nanofiltration membranes treating perfluorooctane sulfonate containing wastewater, *Environ. Sci. Technol.* 41 (6) (2007) 2008–2014.